Strain disorder and gapless intervalley coherent phase in twisted bilayer graphene

Gal Shavit, Kryštof Kolář, Christophe Mora, Felix von Oppen, and Yuval Oreg

Phys. Rev. B **107**, L081403 — Published 9 February 2023

DOI: 10.1103/PhysRevB.107.L081403

Strain Disorder and Gapless Intervalley Coherent Phase in Twisted Bilayer Graphene

Gal Shavit,[1] Kryštof Kolář,[2] Christophe Mora,[3] Felix von Oppen,[2] and Yuval Oreg[1]

[1]*Department of Condensed Matter Physics, Weizmann Institute of Science, Rehovot, Israel 7610001*
[2]*Dahlem Center for Complex Quantum Systems and Fachbereich Physik, Freie Universität Berlin, 14195 Berlin, Germany*
[3]*Université Paris Cité, CNRS, Laboratoire Matériaux et Phénomènes Quantiques, 75013 Paris, France*

Correlated insulators are frequently observed in magic angle twisted bilayer graphene at even fillings of electrons or holes per moiré unit-cell. Whereas theory predicts these insulators to be intervalley coherent excitonic phases, the measured gaps are routinely much smaller than theoretical estimates. We explore the effects of random strain variations on the intervalley coherent phase, which have a pair-breaking effect analogous to magnetic disorder in superconductors. We find that the spectral-gap may be strongly suppressed by strain disorder, or vanish altogether, even as intervalley coherence is maintained. We discuss predicted features of the tunneling density of states, show that the activation gap measured in transport experiments corresponds to the diminished gap, and thus offer a solution for the apparent discrepancy between the theoretical and experimental gaps.

Introduction.—In recent years, magic-angle twisted bilayer graphene (MATBG) [1] has emerged as an exciting and versatile platform for strong-correlation physics. Its rich phase diagram prominently features correlated insulators, Chern insulators, superconductivity, and strange metallicity [2–12].

Correlated insulators consistently found at fillings $\nu = \pm 2$ electrons per moiré unit cell relative to charge neutrality (CN), and more rarely at CN, have been suggested to originate from Kramers intervalley-coherent order (K-IVC) [13–16]. The K-IVC phase is in some sense analogous to a superconductor, with the condensate made up of intervalley electron-holes pairs. Interestingly, theoretical predictions of the K-IVC gap energy, by both Hartree-Fock and numerically exact methods, overestimate the measured activation gap of $\sim \mathcal{O}(1\,\mathrm{meV})$ [2, 4–6, 9] by more than an order of magnitude.

It has been experimentally well-established that the moiré lattice formed in realistic MATBG devices is not pristine, presumably due to substantial relaxation effects of the underlying graphene lattice [17]. Disorder in the local twist angle between the graphene layers has been observed [7, 18], leading to domains with slightly different effective moiré unit-cell sizes. Local measurements have also shown significant strain effects, consistent with a moiré lattice distortion of $0.1\% - 0.7\%$ [19–21].

As the two graphene layers may be subjected to different strain fields, the strain tensor applied to the bilayer is comprised of a layer-symmetric part (homostrain) and a layer-antisymmetric contribution (heterostrain). Uniform heterostrain was suggested to have an important role in weakening the even-filling correlated insulator states in MATBG [13, 22]. This is mainly due to a large increase of the flat-bands bandwidth [23, 24], leading to diminished effective interactions.

Whereas heterostrain shifts the two Dirac points within each valley with respect to each other, homostrain subjects both layers to identical distortions and mainly acts as a pseudo-gauge field. This field acts oppositely in the two valleys (as illustrated in Fig. 1a), thus maintaining time-reversal symmetry (TRS). In this manuscript, we explore the effects of spatially random homostrain (Fig. 1b) on the properties of the K-IVC phase. We show that this perturbation induces "pair-breaking" effects in striking resemblance to magnetic impurities in spin-singlet superconductors. Effects of other types of strain on the K-IVC phase are discussed in the supplementary materials (SM) [25], and various disorder perturbations are classified by their impact on this phase in Ref. [26].

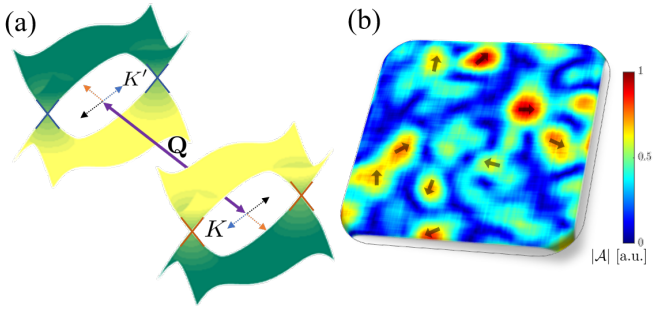

FIG. 1. Schematic description of our model. (a) The band structure in each valley (K, K') is approximated by two Dirac cones, one in each "mini-valley". The momentum separating the valleys, $\mathbf{Q}$, is modified by random homostrain fluctuations acting on the graphene layers, as represented by colored dotted arrows. (b) Schematic of a possible random strain configuration. Color indicates the strain strength $|\boldsymbol{\mathcal{A}}|$, whereas arrows indicate the directions of the local distortions of the graphene lattice.

We find that modest strain fluctuations reduces both the K-IVC order parameter (OP) and the spectral-gap, but enable the two to be dramatically different from one another. We propose that this effect may be responsible for the surprisingly small activation gap observed in transport experiments. Moreover, we show that intervalley coherence can persist even when the system becomes gapless to single-particle excitations, a phase that we dub "gapless K-IVC". This phase could explain the haphazard appearance of a correlated insulator at CN.

Model.—We consider the following simplified spinless model of MATBG,

$$H_0 = \sum_{\mathbf{k}} \Psi^\dagger_{\mathbf{k}} \left[u k_x \sigma_x \tau_z + u k_y \sigma_y \right] \Psi_{\mathbf{k}}, \tag{1}$$

where $\Psi^\dagger_{\mathbf{k}}$ is an 8-spinor of fermionic annihilation operators at momentum $\mathbf{k}$ relative to their respective origin in momentum space, and with sublattice, valley, and "mini-valley" degrees

of freedom, described by Pauli matrices σ_i, τ_i, and ρ_i, respectively. This model features four Dirac cones with linear dispersion $\epsilon_{\mathbf{k}} = \pm u\,|\mathbf{k}|$. H_0 preserves the TRS $\mathcal{T} = \tau_x\rho_x\mathcal{K}$ ($\mathcal{K}$ implements complex conjugation), with $\mathcal{T}^2 = 1$.

The spinless model effectively describes the fillings $\nu = \pm 2$, where two electronic flavors of opposite valleys are entirely filled or empty, while the remaining pair is "active" and forms intervalley coherence. Conversely, two copies of our spinless model may be used describe the K-IVC phase at CN [13–16].

We introduce local density-density repulsive interactions,

$$H_{\text{int}} = \frac{U}{2\Omega}\sum_{\mathbf{k},\mathbf{k}',\mathbf{q}} \Psi^{\dagger}_{\mathbf{k}+\mathbf{q}}\Psi_{\mathbf{k}}\Psi^{\dagger}_{\mathbf{k}'-\mathbf{q}}\Psi_{\mathbf{k}'}, \tag{2}$$

which induce spontaneous symmetry-breaking in our model on a mean-field level. (Ω is the system area.) This simplified form of H_{int} suffices to illustrate the phenomenon we are interested in. Specifically, we examine the K-IVC phase, which has been argued to be the likely ground state of MATBG at even fillings. The K-IVC state is characterized by intervalley coherence, i.e., formation of an exciton condensate with intervalley electron-hole pairs, a finite gap to charge excitations, and TRS breaking. The corresponding mean-field Hamiltonian at a given $\mathbf{k}$ has the form

$$h_{\text{MF}}(\mathbf{k}) = u\,(k_x\sigma_x\tau_z + k_y\sigma_y) + \Delta_{\text{ivc}}\sigma_x\tau_x\rho_z. \tag{3}$$

h_{MF} preserves a Kramers-like TRS, $\mathcal{T}' = \tau_y\rho_x\mathcal{K}$, which concatenates $\mathcal{T}$ with a valley rotation. It also preserves chiral and particle-hole symmetries, represented by $\mathcal{S} = \sigma_z$ and $\mathcal{C} = \mathcal{S}\mathcal{T}'$, respectively [27] .

We now introduce random homostrain variations, which enter the model as a random gauge field acting in opposite directions in opposite valleys, see Fig. 1b. Concretely, the strain Hamiltonian may be written as

$$H_{\text{str}} = u\int d\mathbf{r}\Psi^{\dagger}(\mathbf{r})\left[\mathcal{A}_x(\mathbf{r})\,\sigma_x + \mathcal{A}_y(\mathbf{r})\,\sigma_y\tau_z\right]\Psi(\mathbf{r}), \tag{4}$$

where $\boldsymbol{\mathcal{A}}$ is the strain-induced perturbation, and $\Psi(\mathbf{r}) = \frac{1}{\sqrt{\Omega}}\sum_{\mathbf{k}} e^{i\mathbf{k}\cdot\mathbf{r}}\Psi_{\mathbf{k}}$. In Eq. (4) we have implicitly assumed that the strain potential is smooth on the moiré length scale. Otherwise one should replace the renormalized velocity u by the much larger bare graphene Fermi velocity v_F. Notice that uniform strain constitutes a shift of $\mathbf{k}$ in H_0 [28] and redefines the momentum connecting the two valleys $\mathbf{Q} = \mathbf{K} - \mathbf{K}'$. This only changes the momentum carried by the condensed electron-hole K-IVC pairs, so that we can assume $\mathcal{A}_i$ has zero spatial mean.

The perturbation in Eq. (4) does not break any of the symmetries of h_{MF}. However, as we will show below (see also Ref. [26]), the fact that it commutes with the K-IVC operator $\sigma_x\tau_x\rho_z$, enables a drastic reduction of the gap which opens in the K-IVC spectrum due to the random strain disorder. For this reason, we have also neglected inter-minivalley scattering, which have additional ρ_x, ρ_y factors, and thus anticommute with the OP.

Considering a simple point-like perturbation, $\boldsymbol{\mathcal{A}}(\mathbf{r}) = \boldsymbol{\mathcal{A}}_0\delta(\mathbf{r})$, one may employ a T-matrix formalism to find the bound-state spectrum inside the mean-field gap [25], in analogy to Yu-Shiba-Rusinov states induced by magnetic impurities in a superconductor [29–31]. We find that as the perturbation strength increases, the in-gap-state energy is reduced and the two bound-state energies cross at zero when the impurity strength becomes an appreciable fraction of the bandwidth W.

Moreover, we find that when approximating the density-of-states (DOS) as a constant around the Fermi level (rather than linear as appropriate in our case), one recovers – apart from additional degeneracies – precisely the bound-state spectrum of a magnetic impurity inside a singlet superconductor. This outcome may be traced to the analogous algebraic structure of the two problems, i.e., the impurity operator commuting with the OP. This analogy enables the treatment of random strain fluctuations in MATBG by tools similar to those employed in superconductors with magnetic impurities.

Abrikosov-Gor'kov approach.—We therefore treat the random strain fluctuations within the self-consistent Born approximation (SCBA), inspired by the Abrikosov-Gor'kov theory of superconductivity in magnetically disordered alloys [32]. A similar method was also used to study exciton condensates in the presence of potential impurities [33, 34].

The main object of interest is the Green's function,

$$G(\mathbf{k},\omega) = \left(i\omega - h_{\text{MF}} - \hat{\Sigma}_{\text{SCBA}}\right)^{-1}. \tag{5}$$

Within the SCBA, the self-energy matrix $\hat{\Sigma}_{\text{SCBA}}$ can be written as

$$\hat{\Sigma}_{\text{SCBA}}(\mathbf{k},\omega) = \left\langle \sum_{\mathbf{p}} \mathcal{U}_{\mathbf{k}-\mathbf{p}} G(\mathbf{p},\omega)\,\mathcal{U}_{\mathbf{p}-\mathbf{k}} \right\rangle_{\text{dis.}}, \tag{6}$$

where the matrix $\mathcal{U}$ represents the random strain perturbation in momentum space, $H_{\text{str}} = \sum_{\mathbf{kq}} \Psi^{\dagger}_{\mathbf{k}+\mathbf{q}}\mathcal{U}_{\mathbf{q}}\Psi_{\mathbf{k}}$, and $\langle\ldots\rangle_{\text{dis.}}$ stands for disorder averaging.

Manipulating the Green's function, it can be written as

$$G = -\frac{i\tilde{\omega} + u\,(k_x\sigma_x\tau_z + k_y\sigma_y) + \tilde{\Delta}\sigma_x\tau_x\rho_z}{\epsilon^2_{\mathbf{k}} + \tilde{\Delta}^2 + \tilde{\omega}^2}. \tag{7}$$

The parameters $\tilde{\omega}, \tilde{\Delta}$ are related to $\omega, \Delta_{\text{ivc}}$ by the self-consistency equations

$$\begin{pmatrix}\tilde{\omega}\\ \tilde{\Delta}\end{pmatrix} = \begin{pmatrix}\omega\\ \Delta_{\text{ivc}}\end{pmatrix} + \Gamma\mathcal{F}\left(\tilde{\omega},\tilde{\Delta}\right)\begin{pmatrix}\tilde{\omega}\\ -\tilde{\Delta}\end{pmatrix}, \tag{8}$$

where $\mathcal{F}\left(\tilde{\omega},\tilde{\Delta}\right) = \frac{W}{2}\int d\epsilon \frac{\mathcal{N}(\epsilon)}{\epsilon^2+\tilde{\Delta}^2+\tilde{\omega}^2}$, $\mathcal{N}(\epsilon)$ is the DOS per unit-cell of area $\Omega_{u.c.}$, and W is the bandwidth. The disorder energy scale Γ is

$$\Gamma = \frac{2\Omega}{W\Omega_{u.c.}}\left\langle \int d\theta u^2 \mathbf{A}^{\dagger}_{\theta}\cdot\mathbf{A}_{\theta}\right\rangle_{\text{dis.}}, \tag{9}$$

where $\mathbf{A}_{\mathbf{q}}$ is the Fourier transform of $\boldsymbol{\mathcal{A}}(\mathbf{r})$, and we have used the standard approximation that the scattering mostly depends on the angle between incoming and outgoing momenta

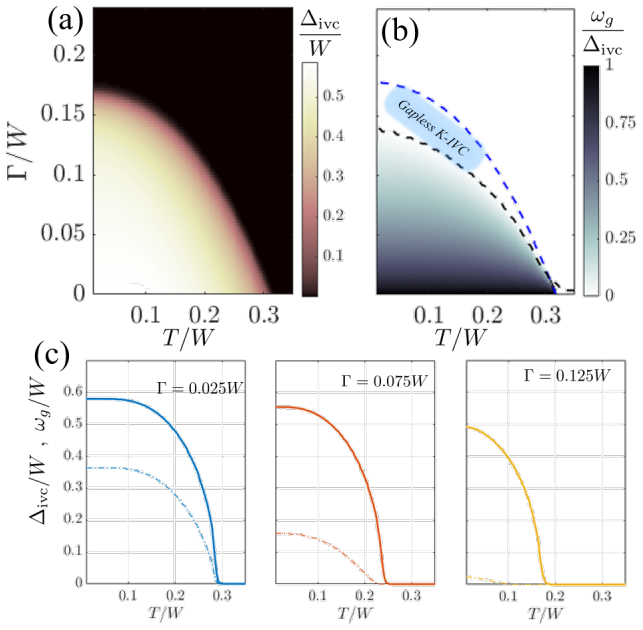

FIG. 2. (a) The OP $\Delta_{\rm ivc}$ as a function of temperature and disorder energy scale Γ. For a given temperature, there is a critical Γ at which the OP vanishes. (b) The ratio between the gap in the TDOS, ω_g, and $\Delta_{\rm ivc}$. As Γ increases, ω_g deviates from $\Delta_{\rm ivc}$ appreciably. There exists a gapless K-IVC region bounded by the vanishing of the single-particle gap (black dashed line) and of the OP (blue dashed line). We used $U = 0.7W$ and a linear DOS $\mathcal{N}_{\rm lin.}$. (c) Linecuts for different values of Γ showing $\Delta_{\rm ivc}$ (solid) and ω_g (dash-dotted).

θ [33, 34]. As for magnetic impurities in superconductors and potential scatterers in excitonic condensates, the form of Eq. (8) is due to the K-IVC OP commuting with the random perturbation. Thus, the equations we find are identical to the Abrikosov-Gor'kov equations for superconductors with magnetic impurities, with one important difference. In MATBG, we cannot assume a constant DOS near the Fermi energy, but should account for the fact that the DOS *vanishes linearly* at the Dirac point. This leads to important qualitative differences in the results.

By relating the local strain to the effective gauge-field $\boldsymbol{\mathcal{A}}$, one may obtain an order-of-magnitude estimate of Γ. For root-mean-square strains of $\mathcal{E} \sim 0.1\%$ and disorder correlation lengths of few unit cells, we find Γ/W values of $0.1-0.3$ [25]. As will be shown, such values are sufficient to dramatically reduce the spectral-gap or even close it completely.

The strength of K-IVC order in the presence of disorder is obtained by combining Eq. (8) with the gap equation

$$\Delta_{\rm ivc} = -2\frac{U}{\beta\Omega}\sum_{\omega\mathbf{k}} \mathrm{Tr}\left\{\sigma_x\tau_x\rho_z G\right\}, \qquad (10)$$

which we solve numerically. (Here, β is inverse temperature.) Figure 2a shows results for the OP $\Delta_{\rm ivc}$ as a function of temperature and disorder. We find that both the OP and the critical temperature deteriorate with increasing disorder.

Assuming a DOS which is linear in energy, $\mathcal{N}_{\rm lin.} = 4|\epsilon|/W^2$ with cutoff energy $|\epsilon| < W/2$, we can also make analytical progress. In particular, we calculate the critical disorder scale Γ_c, at which $\Delta_{\rm ivc}$ vanishes for $T = 0$. In the regime $\Gamma_c \ll W/2$, we find [25]

$$\Gamma_c = \frac{U_c}{\log 8}\left(1 - \frac{U_c}{U}\right), \qquad (11)$$

where $U_c = W/4$ is the critical interaction U below which the K-IVC order vanishes at $\Gamma, T = 0$. The finite U_c as well as the form of the critical "pair-breaking" parameter Γ_c originate in the DOS vanishing linearly at zero. This suppresses the analog of the Cooper-instability for arbitrarily-weak interactions, which requires finite DOS at the Fermi level.

Having found the self-consistent Green's function, we can calculate the tunneling density-of-states (TDOS) $\tilde{\mathcal{N}}(\epsilon) = \frac{1}{\pi}\mathrm{Im}\frac{1}{\Omega}\sum_{\mathbf{k}}\mathrm{Tr}G(\mathbf{k}, \omega \to i\epsilon)$. In clean systems, the gap ω_g in the TDOS is equal to the OP $\Delta_{\rm ivc}$. In the presence of finite disorder, ω_g is in general smaller than $\Delta_{\rm ivc}$.

In Fig. 2b, we plot the ratio $\omega_g/\Delta_{\rm ivc}$. As Γ increases, this ratio gradually deviates from unity, eventually reaching zero, *before* $\Delta_{\rm ivc}$ vanishes. We dub the regime with finite $\Delta_{\rm ivc}$ and vanishing ω_g as the gapless K-IVC phase. Similar to gapless superconductivity, we interpret this regime as one where intervalley coherence exists throughout a large fraction of the system, yet strain-induced in-gap states form a low-energy compressible continuum of states. For linear DOS, we find that the disorder strength at which the gap closes is related to $\Delta_{\rm ivc}$ [25] through $\Gamma_g = W/\log\left(1 + \frac{W^2}{\Delta_{\rm ivc}^2}\right)^2$.

In Fig. 2c, we plot linecuts of Fig. 2a for several values of Γ. We find that even for modest (and realistic) disorder strengths, the spectral-gap is significantly suppressed compared to the naive gap as given by the OP. Thus, devices which host appreciable strain fluctuations may exhibit an effective gap as seen in a global transport measurement, which is about an order of magnitude smaller than the expected condensation OP.

In Fig. 3 we track the evolution of the TDOS with disorder strength. At very low Γ we find two narrow K-IVC bands separated by roughly $2\Delta_{\rm ivc}$, as expected from previous theoretical investigations of the pristine K-IVC phase. As the disorder strength Γ increases, these bands spread out in energy, and their separation diminishes. This is very different from the behavior of $\Delta_{\rm ivc}$. While ω_g diminishes already for weak disorder, $\Delta_{\rm ivc}$ remains mostly unaffected up to intermediate values of Γ.

The TDOS depicted in Fig. 3 can be measured in planar tunneling junctions with a large tunneling area, similar to the experimental verification of gapless superconductivity [35]. The large tunneling area is required for effective averaging over disorder configurations in a particular device. Such measurements are expected to show two spread-out TDOS lobes, with centers separated by $\sim 2\Delta_{\rm ivc}$ and a spectral-gap of $2\omega_g < 2\Delta_{\rm ivc}$. In contrast, local scanning-tunneling-microscopy (STM) measurements do not reveal disorder-averaged quantities, yet we expect the tunneling gap to vary

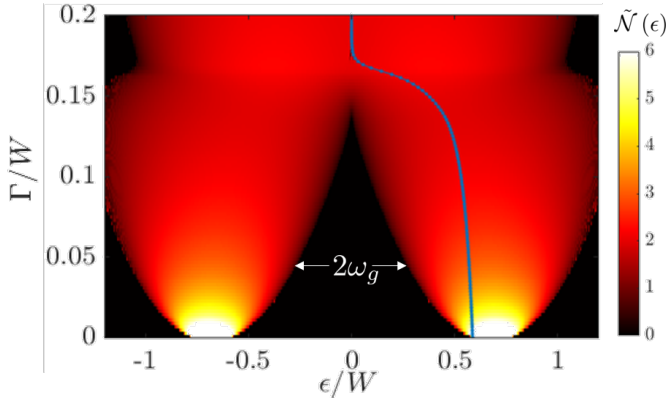

FIG. 3. Evolution of the TDOS $\tilde{\mathcal{N}}(\epsilon)$ with Γ. The gap ω_g gradually closes as the disorder strength increases. Blue line indicates evolution of $\Delta_{\rm ivc}/W$ with increasing Γ. Notice its evolution differs from that of the single-particle gap as it deteriorates more slowly. We used $U = 0.7W, T = 0$.

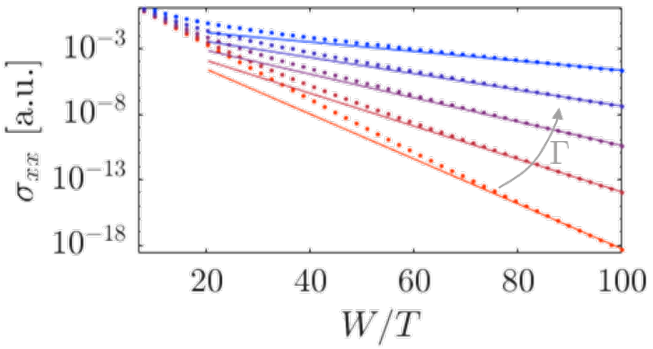

FIG. 4. Calculated DC conductivity σ_{xx}. Dots: σ_{xx} as a function of temperature for different strengths of the strain fluctuations, $\Gamma/W \in [0.02, 0.1]$, increasing from bottom (red) to top (blue) in steps of 0.02. We used the same parameters as in Fig. 2. Solid lines: guides to the eye $\propto \exp\left[-\omega_g\left(T \to 0\right)/T\right]$ for each Γ value. Whereas ω_g differs by a factor of ~ 5 between the first and last plots, $\Delta_{\rm ivc}$ changes only modestly by $< 25\%$.

as a function of position, in a manner correlated with the homostrain variations. Such phenomenology would be a clear indicator of the proposed disordered K-IVC phase.

To make contact with transport experiments, we now turn to calculating the DC conductivity. We use the Kubo-Bastin formula [36], $\sigma_{xx} \propto \int d\epsilon \left(-\frac{df}{d\epsilon}\right) \mathcal{S}(\epsilon)$, where f is the Fermi function, and

$$\mathcal{S}(\epsilon) \approx \frac{1}{\Omega} \sum_{\mathbf{k}} \mathrm{Tr}\left\{ j_x \mathrm{Im}G\left(\mathbf{k}, \omega \to i\epsilon\right) j_x \mathrm{Im}G\left(\mathbf{k}, \omega \to i\epsilon\right) \right\} \tag{12}$$

is the conductivity kernel. The current operator is $j_x = u\sigma_x\tau_z$. Equation (12) neglects vertex corrections to j_x, which may have quantitative significance, but are beyond the scope of this work.

Fig. 4 presents Arrhenius plots of the conductivity for different Γ values. We can extract the activation energy $E_{\rm act}$ by fitting the conductivity to $\sigma_{xx} \propto \exp\left(-E_{\rm act}/T\right)$. Remarkably, we observe that the low-T behavior is indeed temperature activated with $E_{\rm act} \approx \omega_g$, and not the potentially-much-larger $\Delta_{\rm ivc}$. (In the topmost plot of Fig. 4 $\Delta_{\rm ivc} \approx 5.4\omega_g$.) This behavior can be traced to the analytic structure of $\mathcal{S}(\epsilon)$, which has a gap $\approx 2\omega_g$ around $\epsilon = 0$ [25], similar to the TDOS.

Conclusions.—We have explored the consequences of random homostrain fluctuations on the K-IVC state, believed to describe the insulating phases of MATBG at even fillings. Using a simplified model for MATBG, we have studied this problem using the SCBA in conjunction with a mean-field treatment of the K-IVC OP. Homostrain disorder has a pair-breaking effect on the intervalley coherent condensate, since it locally acts on the two valleys in opposite ways.

In contrast to similar pair-breaking disorder problems, random homostrain does not break any symmetries of the K-IVC state. However, it does lead to in-gap states, gap closing, and OP deterioration due to its operator structure – it commutes with the OP. Moreover, the DOS dependence on energy had to be taken into account, since it vanishes at the Dirac point. This led to the unique form of the solutions of the Abrikosov-Gor'kov equations which we derive, and of the critical pair-breaking parameter Γ_c.

One of our key results is the significant separation between the energy scales of the K-IVC order ($\Delta_{\rm ivc}$) and the spectral-gap for single-particle excitations (ω_g), even for modest values of disorder. Borrowing insights from superconductors, the gap reduction stems from in-gap bound states, which become stronger and more abundant with increasing Γ, yet impact the surrounding intervalley-coherent condensate only weakly.

We suggest that the order-of-magnitude discrepancy between the theorized K-IVC gap and the activation gap measured in transport experiments can be resolved within our model. We have demonstrated that the relevant activation energy as measured via the DC conductivity is the spectral-gap, which may be considerably smaller than the OP due to disorder. (Both scales coincide in the pristine case). The rare appearance of insulators at CN can also be understood by considering two copies of our model with different spin labels. Variations of the magnitude of strain disorder between devices may tip the state at CN from a weakly-insulating K-IVC state to the gapless K-IVC regime. The relative weakness of the insulating state at CN compared to fillings $\nu = \pm 2$ has been attributed to bandwidth renormalizations [37–39], rendering the effective interactions stronger away from CN.

The interplay of strain fluctuations with other sources of K-IVC suppression, such as twist-angle disorder and uniform heterostrain, remains to be explored. Additionally, the fact that the considered disorder couples only to intervalley-ordered states may also be important. This may have ramifications for the competition between the K-IVC state and other correlated insulating phases, such as the valley-Hall phase, for which the OP $\propto \sigma_z$ anticommutes with the strain fluctuations. Incorporating such complications, as well as including more intricate aspects of the (particle-hole asymmetric) band structure will shed much-needed light on the nature of the insulat-

ing phases in MATBG and their variation between different devices.

We gratefully acknowledge funding by Deutsche Forschungsgemeinschaft through CRC 183 (project C02; YO and FvO), a joint ANR-DFG project (TWISTGRAPH; CM and FvO), the European Union's Horizon 2020 research and innovation program (Grant Agreement LEGOTOP No. 788715; YO), the ISF Quantum Science and Technology program (2074/19; YO), and a BSF and NSF grant (2018643; YO).

[1] R. Bistritzer and A. H. MacDonald, Proc. Nat. Acad. Sci. **108**, 12233 (2011).
[2] Y. Cao, V. Fatemi, A. Demir, S. Fang, S. L. Tomarken, J. Y. Luo, J. D. Sanchez-Yamagishi, K. Watanabe, T. Taniguchi, E. Kaxiras, R. C. Ashoori, and P. Jarillo-Herrero, Nature **556**, 80 (2018).
[3] Y. Cao, V. Fatemi, S. Fang, K. Watanabe, T. Taniguchi, E. Kaxiras, and P. Jarillo-Herrero, Nature **556**, 43 (2018).
[4] X. Lu, P. Stepanov, W. Yang, M. Xie, M. A. Aamir, I. Das, C. Urgell, K. Watanabe, T. Taniguchi, G. Zhang, A. Bachtold, A. H. MacDonald, and D. K. Efetov, Nature **574**, 653 (2019).
[5] M. Yankowitz, S. Chen, H. Polshyn, Y. Zhang, K. Watanabe, T. Taniguchi, D. Graf, A. F. Young, and C. R. Dean, Science **363**, 1059 (2019).
[6] Y. Saito, J. Ge, K. Watanabe, T. Taniguchi, and A. F. Young, Nature Phys. **16**, 926 (2020).
[7] U. Zondiner, A. Rozen, D. Rodan-Legrain, Y. Cao, R. Queiroz, T. Taniguchi, K. Watanabe, Y. Oreg, F. von Oppen, A. Stern, E. Berg, P. Jarillo-Herrero, and S. Ilani, Nature **582**, 203 (2020).
[8] D. Wong, K. P. Nuckolls, M. Oh, B. Lian, Y. Xie, S. Jeon, K. Watanabe, T. Taniguchi, B. A. Bernevig, and A. Yazdani, Nature **582**, 198 (2020).
[9] X. Liu, Z. Wang, K. Watanabe, T. Taniguchi, O. Vafek, and J. I. A. Li, Science **371**, 1261 (2021).
[10] G. Chen, A. L. Sharpe, E. J. Fox, Y.-H. Zhang, S. Wang, L. Jiang, B. Lyu, H. Li, K. Watanabe, T. Taniguchi, Z. Shi, T. Senthil, D. Goldhaber-Gordon, Y. Zhang, and F. Wang, Nature **579**, 56 (2020).
[11] M. Serlin, C. L. Tschirhart, H. Polshyn, Y. Zhang, J. Zhu, K. Watanabe, T. Taniguchi, L. Balents, and A. F. Young, Science **367**, 900 (2020).
[12] P. Stepanov, M. Xie, T. Taniguchi, K. Watanabe, X. Lu, A. H. MacDonald, B. A. Bernevig, and D. K. Efetov, Phys. Rev. Lett. **127**, 197701 (2021).
[13] N. Bultinck, E. Khalaf, S. Liu, S. Chatterjee, A. Vishwanath, and M. P. Zaletel, Phys. Rev. X **10**, 031034 (2020).
[14] J. S. Hofmann, E. Khalaf, A. Vishwanath, E. Berg, and J. Y. Lee, Fermionic monte carlo study of a realistic model of twisted bilayer graphene (2021), arXiv:2105.12112.
[15] G. Shavit, E. Berg, A. Stern, and Y. Oreg, Phys. Rev. Lett. **127**, 247703 (2021).
[16] G. Wagner, Y. H. Kwan, N. Bultinck, S. H. Simon, and S. A. Parameswaran, Global phase diagram of twisted bilayer graphene above t_c (2021), arXiv:2109.09749.
[17] N. N. T. Nam and M. Koshino, Phys. Rev. B **96**, 075311 (2017).
[18] A. Uri, S. Grover, Y. Cao, J. A. Crosse, K. Bagani, D. Rodan-Legrain, Y. Myasoedov, K. Watanabe, T. Taniguchi, P. Moon, M. Koshino, P. Jarillo-Herrero, and E. Zeldov, Nature **581**, 47 (2020).
[19] Y. Xie, B. Lian, B. Jäck, X. Liu, C.-L. Chiu, K. Watanabe, T. Taniguchi, B. A. Bernevig, and A. Yazdani, Nature **572**, 101 (2019).
[20] A. Kerelsky, L. J. McGilly, D. M. Kennes, L. Xian, M. Yankowitz, S. Chen, K. Watanabe, T. Taniguchi, J. Hone, C. Dean, A. Rubio, and A. N. Pasupathy, Nature **572**, 95 (2019).
[21] Y. Choi, J. Kemmer, Y. Peng, A. Thomson, H. Arora, R. Polski, Y. Zhang, H. Ren, J. Alicea, G. Refael, F. von Oppen, K. Watanabe, T. Taniguchi, and S. Nadj-Perge, Nature Phys. **15**, 1174 (2019).
[22] D. E. Parker, T. Soejima, J. Hauschild, M. P. Zaletel, and N. Bultinck, Phys. Rev. Lett. **127**, 027601 (2021).
[23] L. Huder, A. Artaud, T. Le Quang, G. T. de Laissardière, A. G. M. Jansen, G. Lapertot, C. Chapelier, and V. T. Renard, Phys. Rev. Lett. **120**, 156405 (2018).
[24] Z. Bi, N. F. Q. Yuan, and L. Fu, Phys. Rev. B **100**, 035448 (2019).
[25] See Supplemental Material including Refs. [40–43] for details regarding strain effects, mean-field approach, local impurity calculations, and the Abrikosov-Gor'kov results.
[26] K. Kolář, G. Shavit, C. Mora, Y. Oreg, and F. von Oppen, Anderson's theorem for correlated insulating states in twisted bilayer graphene (2022), arXiv:2207.11281.
[27] We note that a more realistic model of the band structure of MATBG contains terms which break particle-hole symmetry, as well as terms proportional to τ_z. These break $\mathcal{S}$ and $\mathcal{C}$, reducing the symmetry of h_{MF} from symmetry class CII to AII.
[28] M. Vozmediano, M. Katsnelson, and F. Guinea, Physics Rep. **496**, 109 (2010).
[29] L. Yu, Acta Phys. Sin. **21**, 75 (1965).
[30] H. Shiba, Prog. Theor. Phys. **40**, 435 (1968).
[31] A. I. Rusinov, Zh. Eksp. Teor. Fiz. **9**, 146 (1969), [JETP Lett. 9, 85 (1969)].
[32] A. Abrikosov and L. Gor'kov, Sov. Phys. JETP **8**, 1090 (1959).
[33] J. Zittartz, Phys. Rev. **164**, 575 (1967).
[34] R. Bistritzer and A. H. MacDonald, Phys. Rev. Lett. **101**, 256406 (2008).
[35] M. A. Woolf and F. Reif, Phys. Rev. **137**, A557 (1965).
[36] A. Bastin, C. Lewiner, O. Betbeder-Matibet, and P. Nozieres, J. Phys. Chem. Sol. **32**, 1811 (1971).
[37] M. J. Calderón and E. Bascones, Phys. Rev. B **102**, 155149 (2020).
[38] Z. A. H. Goodwin, V. Vitale, X. Liang, A. A. Mostofi, and J. Lischner, Hartree theory calculations of quasiparticle properties in twisted bilayer graphene (2020), arXiv:2004.14784.
[39] M. Xie and A. H. MacDonald, Phys. Rev. Lett. **127**, 196401 (2021).
[40] A. V. Balatsky, I. Vekhter, and J.-X. Zhu, Rev. Mod. Phys. **78**, 373 (2006).
[41] F. Pientka, L. I. Glazman, and F. von Oppen, Phys. Rev. B **88**, 155420 (2013).
[42] K. Maki, in Superconductivity, Vol. 2, edited by R. D. Parks (Marcel Dekker, 1969) p. 1035.
[43] P. Hirschfeld, D. Vollhardt, and P. Wölfle, Solid State Commun. **59**, 111 (1986).